Acta Oceanol. Sin., 2015, Vol. 34, No. 3, P. 51–58
DOI: 10.1007/s13131-015-0633-8
http://www.hyxb.org.cn
E-mail: hyxbe@263.net

Factors affecting spring bloom in the South of Cheju Island in the East China Sea

FU Dongyang[1]*, HUANG Zhaojun[2], ZHANG Yuanzhi[2], PAN Delu[3], DING Youzhua[1], LIU Dazhao[1], ZHANG Ying[1], MAO Zhihua[3], CHEN Jianfang[3]

[1] Laboratory of Remote Sensing and Information Technology, Guangdong Ocean University, Zhanjiang 524088, China
[2] Shenzhen Research Institute, Chinese University of Hong Kong, Shenzhen, 518057, China
[3] State Key Laboratory of Satellite Ocean Environment Dynamics, Second Institute of Oceanography, State Oceanic Administration, Hangzhou 310012, China

Received 2 July 2014; accepted 11 October 2014

Abstract

A soil circulation occurs in the south of Cheju Island in the spring. Nutrients and its influence on chlorophyll *a* (Chl *a*) around the circulations were studied from April 9 to May 6, 2007. Spring bloom with elevated concentrations of Chl *a* was observed during the investigation. High concentrations of phosphate, nitrate and silicate at 0.6, 12, and 8 mmol/m^3, respectively, were detected. A low water temperature prevented the growth of phytoplankton. Chl *a* concentrations in the study area might be strongly associated with the high silicate concentration.

Key words: phosphate, nitrate, silicate, phytoplankton, circulation

Citation: Fu Dongyang, Huang Zhaojun, Zhang Yuanzhi, Pan Delu, Ding Youzhua, Liu Dazhao, Zhang Ying, Mao Zhihua, Chen Jianfang. 2015. Factors affecting spring bloom in the South of Cheju Island in the East China Sea. Acta Oceanologica Sinica, 34(3): 51–58, doi: 10.1007/s13131-015-0633-8

1 Introduction

The East China Sea (ECS) is one of the most productive parts of the world's oceans, with a total area of 1 249 000 km^2. Owing to the discharge from the Changjiang River (Yangtze River), the intrusions of the Yellow Sea waters, the Taiwan Strait waters, and the Kuroshio waters, as well as the alternating monsoons, the ECS shelf has a complex hydrology (Liu et al., 2003).

In terms of a surface profile, the warm and salty waters from one of Kuroshio branch currents meet the diluted ECS waters influenced by the Changjiang River and form fronts in the ECS (Chen, 2008). Hickox et al. (2000) previously reported that an ocean front in the south of the Cheju Island exists from winter to the following spring from satellite sea surface temperature (SST) data.

For the vertical profile, a local deposit of mud on the south Cheju Island in the ECS was evaluated. Hu (1984) first pointed out that an anticlockwise circulation existed there. Then, Qu and Hu (1993) stated that the mud deposition south of Cheju Island resulted from the bottom Ekman suction of an existing circulation in that area. Yanagi et al. (1996) pointed out that an counterclockwise circulation exists only in the upper layer, whereas a clockwise circulation occurs in the lower layer south of Cheju Island.

Generally, the salinity, and nutrients and chlorophyll *a* (Chl *a*) concentrations show gradients from the coast to offshore areas in the ECS continental shelf (Yu and Xian, 2009). Chen (2008) discussed the summer and winter distributions of nitrogen, phosphate and silicate concentrations in the surface waters of the ECS, and concluded that coastal waters, especially those near the Changjiang Estuary, are higher in nutrient concentrations, whereas offshore waters influenced by the Kuroshio are low in nutrients concentrations and have high temperatures.

Although eddies occurring south of the Cheju Island in the ECS were hardly detected in research studies, these efforts generated information on the hydrological conditions in those regions. Son et al. (2006) examined the vertical distributions of the water temperature, the salinity, the density, and the Chl *a* during spring.

Unfortunately, the distributions of nutrients concentrations were not considered in the study of Son et al. (2006). This study is intended to monitor and identify the main factors controlling the nutrients concentrations distribution south of Cheju Island. An intensive field observation was made in the spring. Moreover, the features of nutrients concentrations distributions were discussed with the concentration of Chl *a* in this paper.

2 Methods

The field observation was made at 30°–32.33°N, 124.33°–127.67°E, across the shelf edge of the East China Sea, as shown in Fig. 1, from April 9 to May 6, 2007. The satellite SST image of

Foundation item: The National Marine Important Charity Special Foundation of China under contract No. 201305019; the National Natural Science Foundation of China under contract No. 41340049; Guangdong Planning of Philosophy and Social Science Funding Projectsunder contract No. GD12YGL04; Foundation for Distinguished Yong Talents in Higher Education of Guangdong under contract No. 2012WYM_0077; the Post-Doctoral Starting Fund of Zhejiang under contract No. BSH1301015; Second Institute of Oceanography, State Oceanic Administration Post-Doctoral Starting Fund of china under contract Nos JG1208 and JG1319; Guangdong Ocean University Doctor Starting Fund of China under contract Nos E11332, E11097 and E12248.

*Corresponding author, E-mail: fdy163@163.com

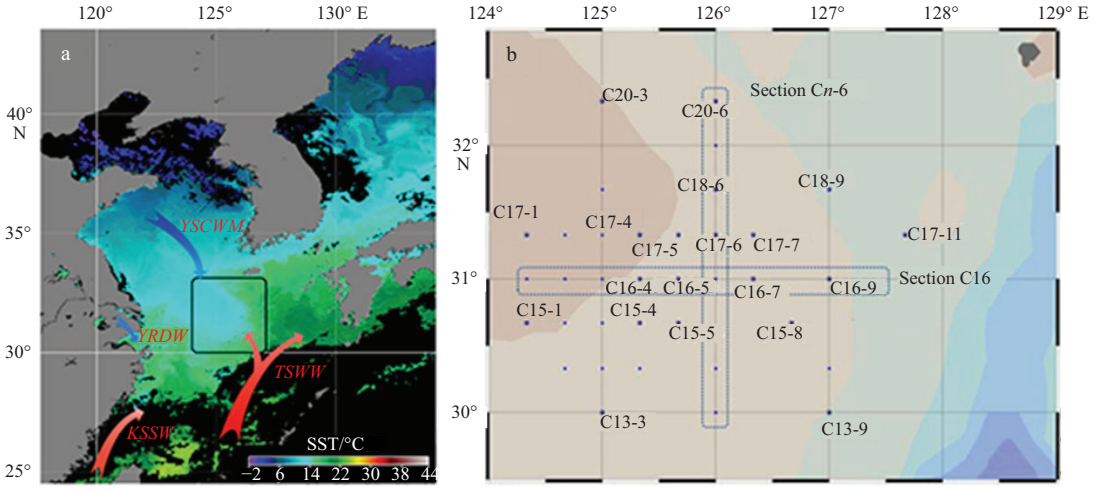

Fig. 1. Standard product of sea surface temperature (SST) image, taken at daytime 11 April 2007 by Aqua MODIS, the study area was marked in the black box. Kuroshio subsurface water (KSSW), Yellow Sea Cold Water Mass (YSCWM), Taiwan Strait warm water (TSWW) and Changjiang River Diluted Water (YRDW) (a); and the detail informations emphasis the change pattern in the study field in the rest of discussion (b).

April 11, 2007 (Fig. 1a) showed that the warm waters of the Tsushima Warm Current flowed into the northern ECS through the southwestern area of Cheju Island. A tongue-shaped pattern extended from the southwestern area of Cheju Island to the shelf area of the northwestern ECS.

The study area and the sampling stations are presented in Fig. 1b (including Sections C13-1 to C13-9, C14-1 to C14-9, C15-1 to C15-8, C16-1 to C16-9, C17-1 to C17-11, C18-1 to C18-9, and Section 20, data losting in part of stations). Two cross-sections, Section C*n*-6 (along transect 126°E) and Section C16 (along transect 31°N) as shown in Fig. 1b, were extensively discussed to present the vertical distribution of particulate nutrients. These two cross-sections typically represented the influence of the Tsushima Currents and Changjiang dilute water, respectively.

Each station was sampled from the surface to the bottom of the sea. The vertical profiles of the temperature and the salinity were measured using a RBR concerto conductivity-temperature-depth (CTD) sensor (RBR Inc., Kanata, Ontario, Canada). The calibration equipment at RBR permits traceable calibration for oceanography instruments, including that for the temperature to ±0.002°C and the conductivity to ±0.003 mS/cm of the accurate values.

Nutrients data, including dissolved inorganic nitrate (DIN), dissolved inorganic phosphates (DIP), and silicate (SiO_3) levels, were acquired using *in-situ* measurements. DIN can be calculated as the sum of nitrate (NO_3^-), nitrite (NO_2^-), and ammonium (NH^{+4}). The concentrations of NO_3^- and SiO_3 which were specified as 0.7% and 6.0% accurate, were measured using a San^{+2} automated wet chemistry analyzer (Skalar Analytical B.V., Netherlands). The concentrations of NO_2^-, NH^{+4}, and PO_4^{-3} were measured by using a spectrophotometer with 8.6%, 14.5%, and 10.0% accuracy, respectively.

Chl *a* was filtered by using a 47 mm GF/F filter, and then extracted by using the 90% acetone, and determined with a Shimadzu UV2401 spectrophotometer (Shimadzu, Inc., Tokyo).

3 Results

Horizontal and vertical distributions of the temperature, the salinity, and the nutrient and chlorophyll *a*, which were measured in the field, are presented in this section. The detailed spatial profiles were drawn by a data-interpolating variational analysis (DIVA) gridding method.

3.1 *Spatial profiles of sea water temperature and salinity*

The horizontal distributions of the temperature at 2, 20, and 40 m below the sea surface obtained from the CTD are presented in Fig. 2. The temperature distribution in three layers was similar to the pattern observed in the MODIS SST image shown in Fig. 1a. Cold water existed in the northwest part of the surface layer and moved downward to the center of the study area 40 m below the sea surface. In addition, water with a temperature being less than 13°C spread from C20-3 to C17-7, in a northwesterly to southeasterly direction. Blocked by the Kuroshio waters, cold water may flow back in a counterclockwise direction; these results were similar to the findings of Yanagi et al. (1996).

The vertical distributions of the water temperature are shown in Fig. 2. A cold water mass with a thickness of approximately 50 m and a temperature less than 13°C existed 20 m below the sea surface. Tawara and Yamagata (1991) previously described that a region with a thickness of approximately 40 m and a temperature less than 13°C existed around 32°N, 126°E.

The horizontal distributions of the salinity are quite dissimilar to those of the temperature. Fresh water exists in the western part of the surface layer, and saline water in the eastern part of the surface layer. The distributions of the water salinity (Fig. 3) showed that fresh water moved from C20-3 to C17-7, in a northwesterly to southeasterly downward direction, which also matched with the observations of Yanagi et al. (1996).

In brief, cold and fresh water could not be transported to 127°E. This may be because the Tsushima Current, a warm branch of the Kuroshio, prevented water from the Yellow Sea to move forward.

3.2 *Spatial profiles of nutrients*

The surface distributions of Si, DIP and DIN concentrations are presented in Fig. 4. The pattern of DIP concentration distribution was comparable with that of DIN. High Si concentration water, which was similar to the pattern indicated in Fig. 4g, extended from the shelf area of the northwestern ECS to the southwestern area of Cheju Island.

High concentrations of DIP and DIN were detected in the

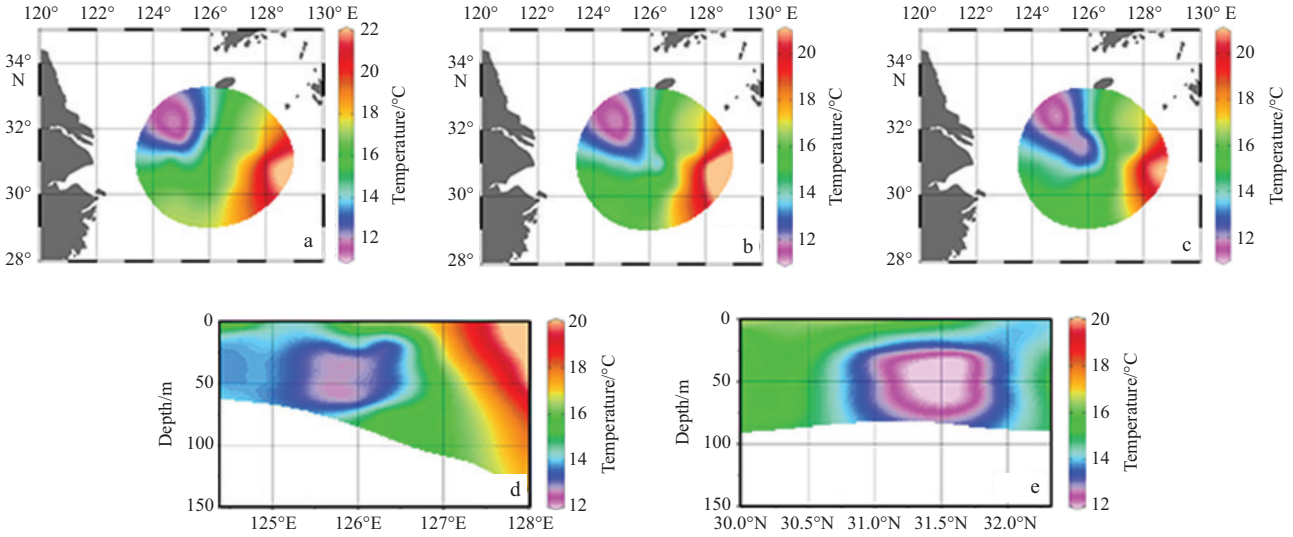

Fig. 2. Contours of water temperature 2 m (a), 20 m (b), and 40 m (c) below the sea surface plotted from data measured using CTD; and the vertical distributions of water temperature at Section C16 (d) and Section C*n*-6 (e).

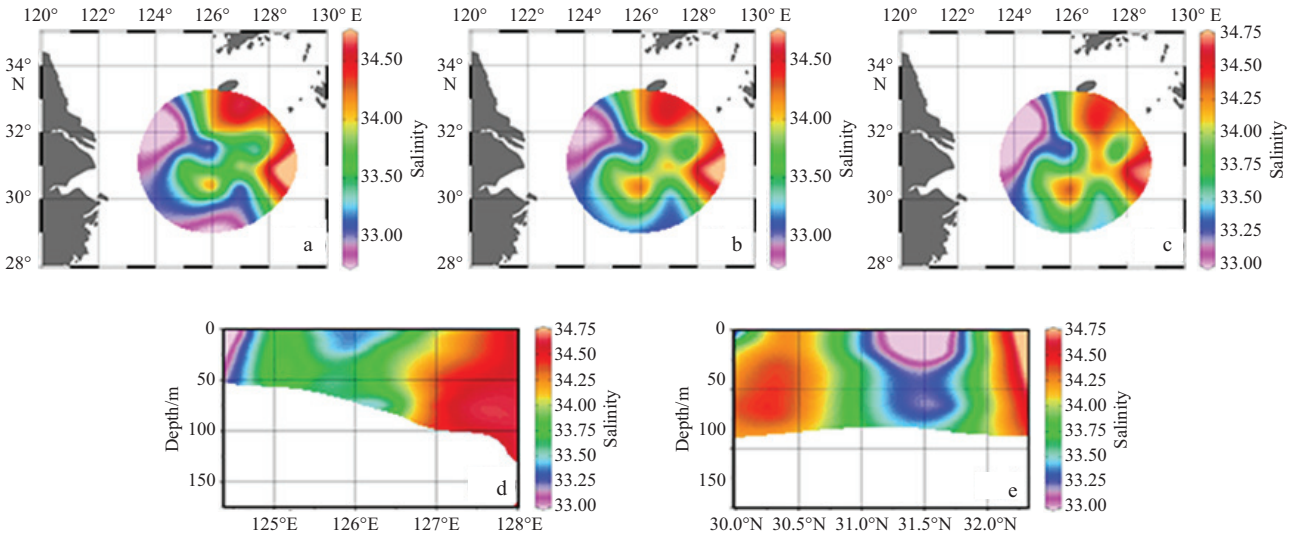

Fig. 3. Contours of salinity 2 m (a), 20 m (b), and 40 m (c) below the sea surface plotted from data measured using CTD; and vertical distributions of salinity at Section C16 (d); and Section C*n*-6 (e).

northwestern part of the surface layer. The highest concentration centers of DIP and DIN could be spotted at 31.7°N, 125°E. Two peaks of silicate concentration were observed at 31.7°N, 125°E and 31°N, 125.7°E.

The concentration distributions of nutrients 20 m below the sea surface have the same distribution patterns as those of the surface layer, although the concentrations of nutrients were higher than the nutrient concentrations at the surface layer. The locations of peak concentrations of nutrients were similar to the locations at the surface layer. The concentration distributions of nutrients 40 m below the sea surface were relatively different from those of the other layers.

Along Transect 126°E, high-nutrient concentration water aggregated under the 20 m water depth from 30.7°N to 31.8°N, and decreased from the bottom to the surface (Fig. 5). It illustrated that nutrients were continuously pulled up from the seabed to the surface. Water columns by 32°N, 126°E are vertically mixed from the surface to the bottom depth, as indicated by Son et al. (1996). Si concentration distributions measured in our studies also showed a similar situation.

3.3 *Spatial profiles of chlorophyll a*

Horizontal concentration distributions of Chl *a* at 2, 20, and 40 m below the sea surface are depicted in Fig. 6. Unfortunately, Chl *a* concentration observations were not conducted at all stations.

The highest concentration of Chl *a* (>10 μg/dm^3) was discovered in the surface layer around Sta. C16-6 (31°N, 126°E), whereas a second peak of Chl *a* concentration was detected at Station C15-2 (30.7°N, 124.7°E). Phytoplankton require multiple nutrients for growth. In the present study, high concentrations of DIN and DIP were observed around 31.7°N, 125°E, but not the near the stations of peak water-column Chl *a* concentrations. Phytoplankton might be driven by Si since a high Chl *a* concentration was observed near the station with high concentration Si.

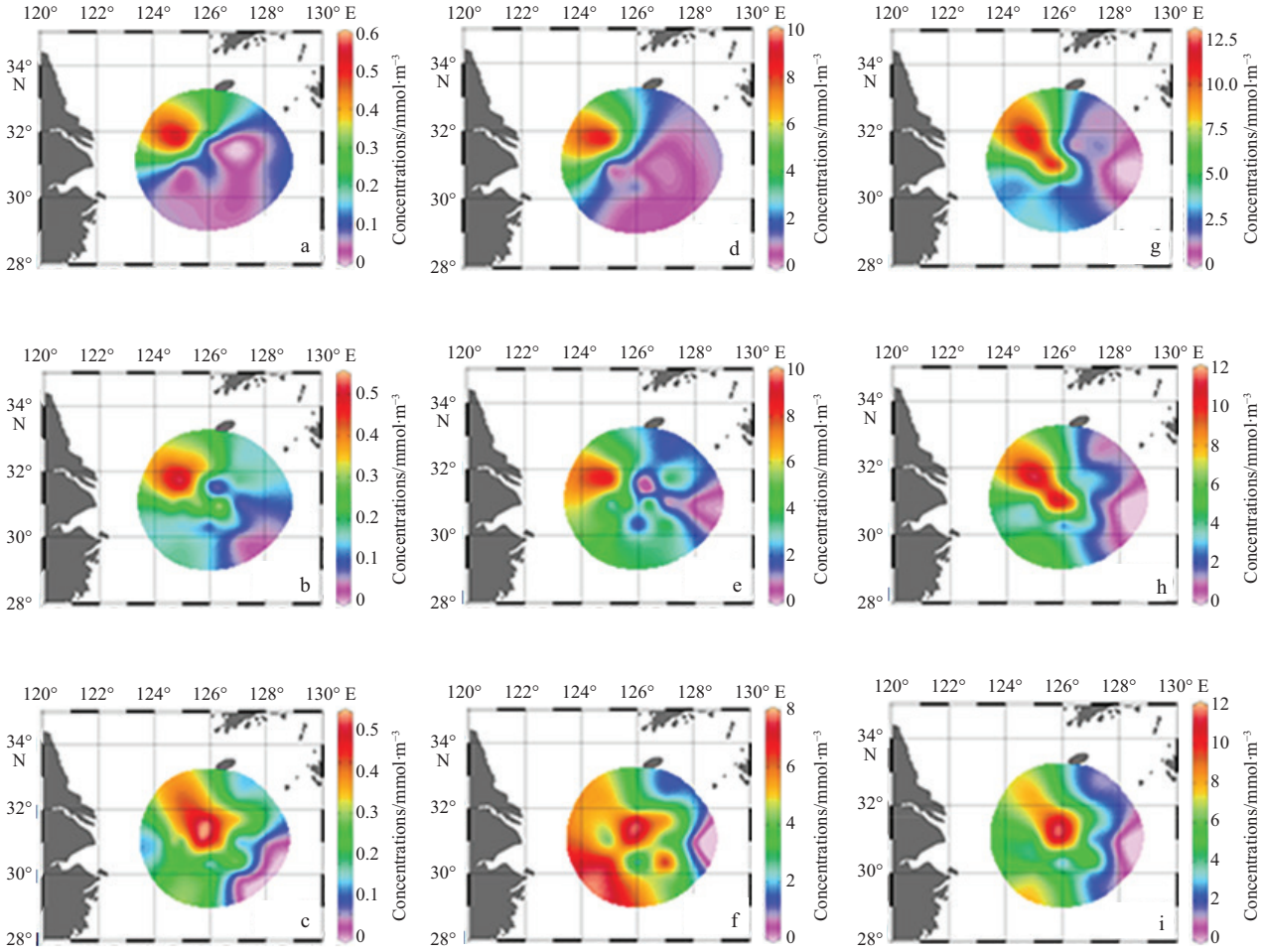

Fig. 4. Horizontal distributions of DIP, DIN and silicate, DIP at 2 m (a), 20 m (b) and 40 m (c); DIN at 2 m (d), 20 m (e), and 40 m (f); silicate at 2 m (g), 20 m (h) and 40 m (i) below the sea surface plotted from data measured using CTD.

The vertical distributions of Chl *a* concentration in Sections C*n*-6 and C16 are shown in Fig. 6. Chl *a* concentrations declined with depth. Phytoplankton were hardly detected 40 m below the sea surface. Water columns with high concentrations of DIN and DIP existed from 20 m water depth to the seabed (Fig. 4). In contrast, phytoplankton gathered from the surface down to 20 m.

4 Discussion

The ocean environment including the nutrients, water temperature, and transparency greatly influences the growth of phytoplankton. Light condition, vertical mixing and phytoplankton sedimentation are the main physical factors that can affect the growth of phytoplankton in the upper layer (Gabric and Parslow, 1989), meanwhile, the water temperature is an important factor affecting the growth of phytoplankton, which influences the Chl *a* concentration by changing the phytoplankton growth and metabolism and other physiological activities (Behrenfeld and Falkowski, 1997; Tang et al., 2006; Hao et al., 2007; Chai et al., 2009), in addition, types of phytoplankton, distribution and structure of nutrients, and remineralization are among the biochemical factors for the growth of phytoplanktons (Klausmeier and Litchman, 2001; Huisman et al., 2006). In the ECS, the Yellow Sea Cold Water Mass (YSCWM), the Changjiang River diluted water (CRDW), the Taiwan Strait warm water (TSWW) and the Kuroshio subsurface water (KSSW) are the important environment fields which have seasonal variations in scale and features (Quan et al., 2013) and determine the biological-environmental relationships (Fig. 1a). In this study, the source of nutrients will be discussed mainly, and then, the key factor of the growth environment will be analyzed using a cluster analysis.

4.1 *Source of nutrients*

In the present study, nutrients were not pushed from inshore to offshore in the CRDW on the surface since the levels of nutrients did not decrease from inshore to offshore. Moreover, the highest concentration of nutrients and a cold water mass (CWM) temperature less than 13°C locating about 50 m below surface (near the bottom) were observed and spread around in the southwest of the Cheju Island in this study (Figs 2 and 4), and this observation is consistent with Yuan et al. (2002) and other researchers (Guo et al., 1995; Yanagi et al., 1996).

Tawara and Yamagate (1991) reported that circulations are expected to occur from early spring until autumn, when the southward spreading of the YSCWM continues, which carry a lots of nutrients into the offshore waters of the ECS. Yanagi et al. (1996) performed an intensive field observation to detect circulations in the same field and observed an counterclockwise circulation in the upper layer, whereas a clockwise circulation occurred in the lower layer south of the Cheju Island. some re-

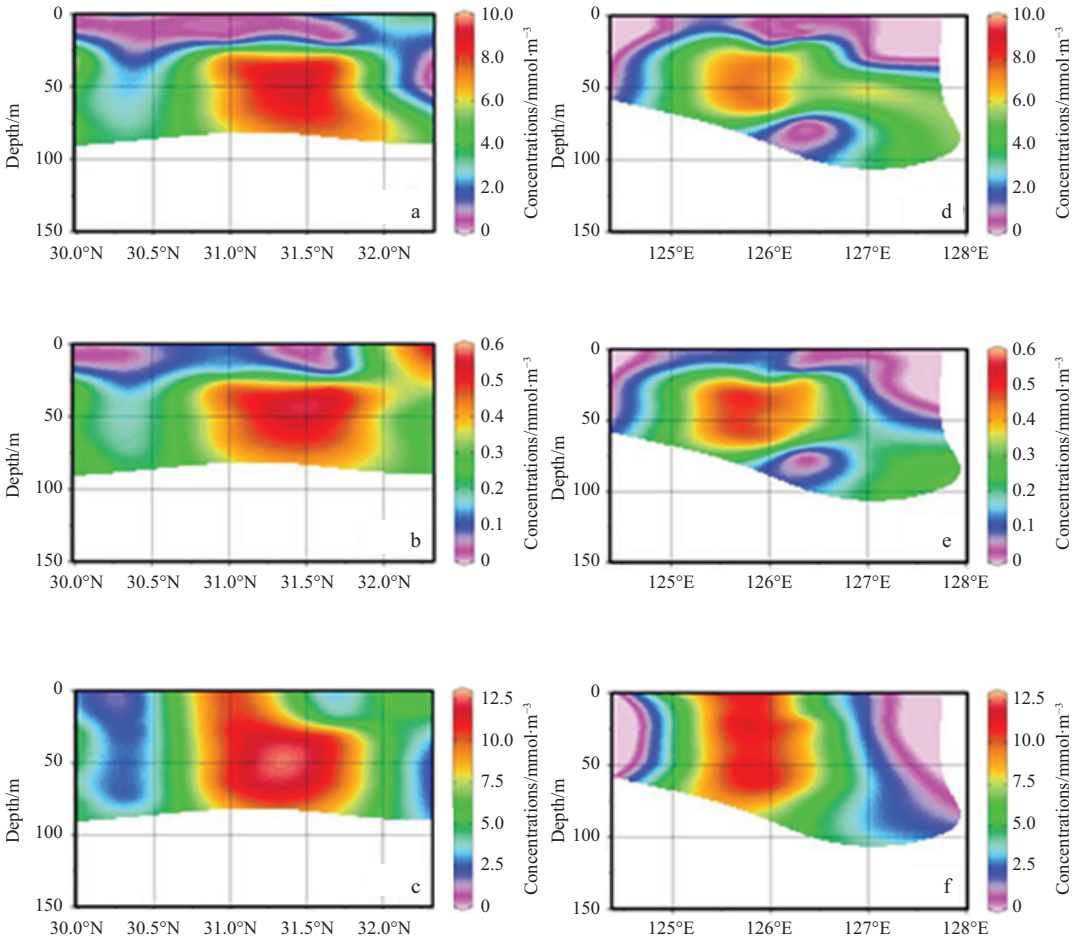

Fig. 5. Vertical distributions of DIN, DIP and silicates concentrations in Section C*n*-6: DIN (a), DIP (b) and silicates (c) and Section C16: DIN (d), DIP (e) and silicates (f).

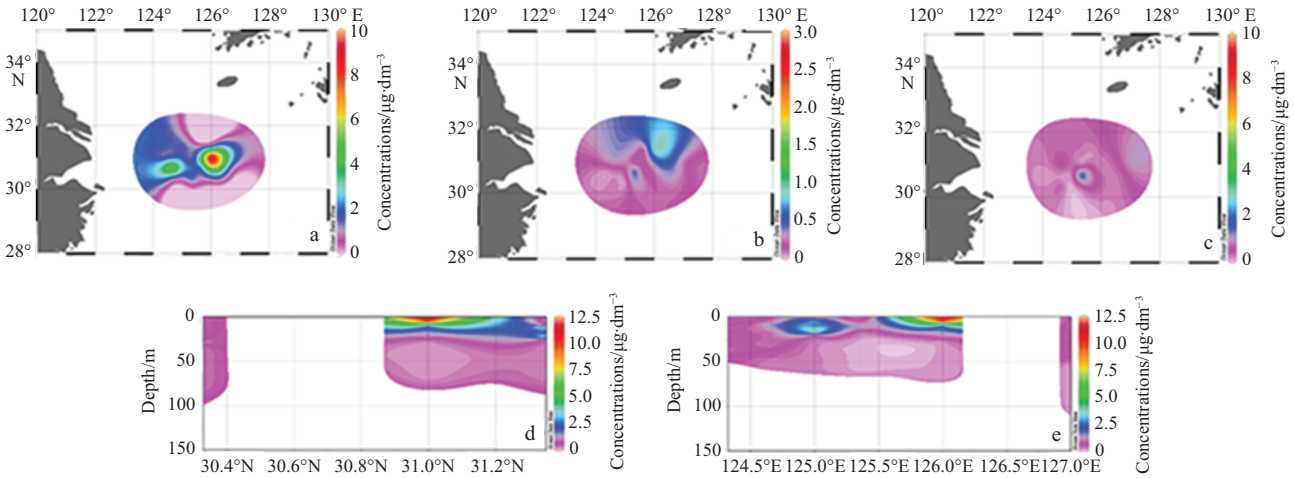

Fig. 6. Contours of Chl *a* concentration 2 m (a), 20 m (b), and 40 m (c) below the sea surface plotted from data measured using CTD. Vertical distributions of chlorophyll a concentration in Section C*n*-6 (d) and Section C16 (e).

searchers pointed out that the CWM was formed by the YSCWM and the CRDW (Qi et al., 1991; Guo et al., 1995), and others by YSCWM and KSSW (Zhou et al., 1990; Lu et al.,1996). In spring, with the arise of the temperature on the upper layer water and appearance of the thermocline, the CWM in the southwest of Cheju Island hold the characteristics of low temperature and mesohaline under the shielding effect of the thermocline (Qi et al., 1991; Li, 1995; Yu et al., 2006) with abundant nutrients with the spreading of the YSCWM.

4.2 *Environmental characteristics*

Phytoplankton require nutrients, light, and appropriate

temperature for growth (Gabric and Parslow, 1989; Behrenfeld and Falkowski, 1997; Tang et al., 2006). Although water transparency data were not collected in the present study, light could be neglected by the analysis of other factors in the surface water since a phytoplankton photosynthesis was not light-limited in the surface water in the outer of the ECS (He et al., 2004). We conducted a cluster analysis of parameters of the Chl *a* and nutrients concentrations, and the temperature, as shown in Table 1.

The cluster analysis was conducted by using Matlab; 16 samples with parameters of and Chl *a*, nutrients concentrations, and the temperature were classified into three major types. Station C18-3 was classified as Type III, and the rest of the stations were classified as Type I and Type II.

Stations C16-5, C16-6, and C16-7 with high Chl *a* concentration levels were grouped together as Type I. These three stations were located close to each other (around 31°N, 126°E) and where a peak in Si concentration levels was observed.

Table 1. Environmental and biological information of the observed stations

Station	Water temperature/°C	Salinity	DIP concentration/ mmol·m^{-3}	Silicate concentration/ mmol·m^{-3}	DIN concentration/ mmol·m^{-3}	Chl *a*/μg·dm^{-3}	Type
C14-3	15.962	33.436	0.03	3.06	1.61	1.528	II
C14-6	16.261	34.219	0.07	1.94	1.47	0.706	II
C14-9	17.788	32.984	0.03	2.15	0.28	0.487	II
C16-1	14.572	33.029	0.19	4.93	4.73	1.584	II
C16-2	15.347	33.225	0.2	5.2	4.36	0.851	II
C16-3	14.428	33.723	0.07	6.42	0.73	2.534	II
C16-5	14.900	33.419	0.09	11.18	1.26	7.145	I
C16-6	16.207	33.392	0.13	10.42	0.61	8.145	I
C16-7	16.297	33.451	0.06	6.95	0.32	6.916	I
C16-9	17.528	33.988	0.02	1.76	0.20	0.580	II
C17-11	17.575	33.345	0.02	1.58	0.66	0.264	II
C17-7	15.845	33.380	0.03	1.92	0.84	2.903	II
C18-3	11.719	32.896	0.55	12.02	8.64	0.891	III
C18-6	15.021	32.949	0.06	3.39	2.36	1.029	II
C18-9	16.939	33.485	0.01	1.65	0.61	0.599	II

The environment around C18-3 was characterized with a low water temperature (11.7°C) and a high concentration level of nutrient, which were features not suitable for the growth of phytoplankton. In contrast, other stations with the environmental characteristics of higher surface-water temperature (ranging from 13.9 to 18.5°C) and nutrients (N, P, and Si) enriched the Chl *a* concentrations.

The cluster analysis indicated that some kind of algal species that can survive in 13.9–18.5°C played an important role in the study area from April to May 2007. The low temperature of the environment might has reduced the consumption rate of nutrients and the growth rate of phytoplankton.

This pattern could be explained by the findings of previous studies. Luo et al. (2007) concluded that Chaetoceros lorenzianus and Bidduphia sinensis Greville could survive in a wider temperature range (12–28°C), which enables them to dominate in the spring in the ECS. Chai et al. (2009) and Tang et al. (2006) also mentioned that Prorocentrum dentatum, which grows well within a temperature range of 20–27°C and grows best in 24°C has become the major algal species in the ECS since the 2000s.

4.3 *Biological-environmental relationships*

The vertical distributions of nutrient concentrations showed that high-nutrient concentration water was continuously pulled up from the bottom to the surface at the tie of circulation. This mode of nutrient supplementation in this area continued in the spring.

The cluster analysis showed that the growth of phytoplankton stopped when the water temperature lower than 12°C. Nutrients might in part affect the phytoplankton growth in the observation field in spring.

The target of this experiment was to find a correlation between phytoplankton and nutrients. A correlation analysis was conducted to establish the relationship between these two variables of Types II and III. Type I was not analyzed in the present study owing to its unclear growth mechanism.

The cluster analysis showed that the illumination and the temperature did not retard the growth of phytoplankton of the Type II cases, which was consistent with our previous analysis, and the growth of phytoplankton was related to some kind of nutrient or ratio between N and P (or silicates) concentrations. Chl *a* concentration data were used as a dependent item in the correlation analysis; the nutrient factors (c_{DIN}:c_{DIP}, c_{DIN}:c_{Si}, DIN concentration, DIP concentration and silicates) measured in sea surface were set as independent items using a 95% confidence interval (n=15). The correlation coefficient between Chl *a* concentration and DIN:DIP was –0.391 7, and that between Chl *a* and c_{DIN}:c_{Si} was –0.526 9, which indicates that the correlations were not significant. A low correlation between Chl *a* and DIN concentrations for the correlation coefficient was –0.224 1. No correlation between Chl *a* and DIP was observed, based on a correlation coefficient of 0.092 9. A high correlation between Chl *a* and silicates concentrations was detected, with a correlation coefficient of 0.865 5 (Fig. 7).

Among the correlation analyses conducted, the linear regression model was used to correlate Chl *a* and silicates concentration.The growth of the phytoplankton was restricted by the type, structure and assimilation of the nutrient (Joseph and Villareal, 1998). Too much deviation of the mole rate of the nutrient in the ocean to the coefficient of the Redfield may be stop the growth of phytoplankton by the lower concentration of the element such as N, P or Si, and affects the species of the phytoplankton in the ocean (Healey and Hendzel, 1980). It is generally acknowledged that the mole rate of $c_{Si} : c_N : c_P$ of the diatom in the ocean is about 16:16:1. In the ECS, as $c_N : c_P$>30, the growth of phytoplankton limited by P, while $c_N : c_P$<8, by N

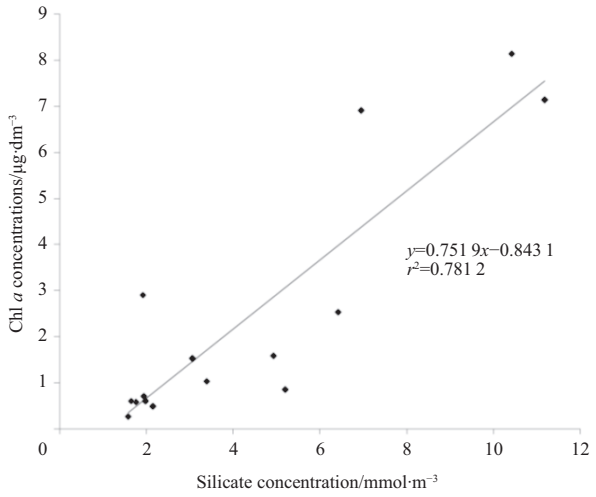

Fig. 7. Relationship between Chl *a* and silicates concentrations can be described as y=0.751 9x–0.843 1, r^2 is the variation of the data explained by the fitted line.

(Hu et al., 1990).

Wang (2003) pointed out that in the ECS, in the spring, the ratio of nitrogen to phosphorus concentration and ratio of silicon to nitrogen concentration were about 15.70 and 4.5, respectively. In this study, the average ratio of nitrogen concentration and ratio of silicon concentration nitrogen one are 22.95 and 4.81, respectively, which are close to the results of Wang (2003). nitrogen and phosphorus in this area in the spring of 2007 were not the restriction factors. As a result, appropriate nitrogen, phosphorus, water temperature and abundant silicon are benefit for the phytoplankton to develop, such as Chaetoceros lorenzianus and Bidduphia sinensis Greville in the ECS in spring (Luo et al., 2007). The relationship with high correlation between Chl *a* and silicon concentrations also indicated that high concentration of nutrients such as silicate may be the cause for phytoplankton to vigorously grow up in the southwest of the Cheju Island in the spring of 2007.

5 Conclusions

The horizontal and vertical distributions of the water temperature, the salinity, and nutrients and Chl *a* concentrations in the circulation area south of Cheju Island during the spring were investigated. The findings of the present study agreed with those of previous studies that the CWM and circulation occurred south of Cheju Island in the spring. The movement of CWM from the Yellow Sea was prevented by a warm branch of the Kuroshio. The circulation could not be distinguished by the SST since the CWM existed 20 m below the sea surface.

Although high nutrients in the water that were brought in by the YSCWM were detected during the observation, the concentration of Chl *a* was relatively low in the relevant area. The cluster analysis result indicated that cold water being less than 12°C could inhibit phytoplankton development.

We also summarized the distribution of nutrients. A high concentration of nutrients existed in the same location of the CWM. In contrast to cold water, nutrients were pulled up to the sea surface by circulation. Interestingly, the increase in Chl *a* upon the circulation in the spring has apparently injected nutrients from bottom to surface. The high correlation between Chl *a* and silicon concentrations followed a linear relationship. Abundant silicon, appreciate nitrogen, phosphorus and the temperature may be the cause of high Chl *a* concentration in the outer of the ECS.

Eddy cores contain nutrient-rich coastal water (Crawford et al., 2005), and eddy dynamics affects spring production, with vertical motion and sloping isopycnals enhancing local and overall production (Liu et al., 2010). Similar to the cold-core eddy in the Luzon Strait (Chen et al., 2007), the eddy cores south of the Cheju Island showed enhanced nutrient levels and high Chl *a* concentrations.

References

Behrenfeld M J, Falkowski P G. 1997. Photosynthetic rates derived from satellite-based chlorophyll concentration. Limnol Oceanogr, 42(1): 1–20

Chai Chao, Yu Zhiming, Shen Zhiliang, et al. 2009. Nutrient characteristics in the Yangtze River Estuary and the adjacent East China Sea before and after impoundment of the Three Gorges Dam. Science of the Total Environment, 407(16): 4687–4695

Chen C T A. 2008. Distributions of nutrients in the East China Sea and the South China Sea connection. Journal of Oceanography, 64(5): 737–751

Chen Y L L, Chen H Y, Lin I I, et al. 2007. Effects of cold eddy on phytoplankton production and assemblages in Luzon Strait bordering the South China Sea. Journal of Oceanography, 63(4): 671–683

Crawford W R, Brickley P J, Peterson T D, et al. 2005. Impact of Haida eddies on chlorophyll distribution in the eastern Gulf of Alaska. Deep-Sea Research Part II: Topical Studies in Oceanography, 52(7–8): 975–989

Gabric A J, Parslow J. 1989. Effect of physical factors on the vertical distribution of phytoplankton in eutrophic coastal waters. Australian Journal of Marine and Freshwater Research, 40(5): 559–569

Guo Zhigang, Yang Zuosheng, Wang Zhaoxiang. 1995. Infuence of water masses on the distribution of sea-floor sediments in the Huanghai Sea and the East China Sea. Journal of Ocean University of Qingdao (in Chinese), 25(1): 75–84

Hao Qiang, Ning Xiuren, Liu Chenggang, et al. 2007. Satellite and in situ observations of primary production in the northern South China Sea. Haiyang Xuebao (in Chinese), 29(3): 58–68

He Xianqiang, Pan Delu, Huang Erhui, et al. 2004. Monitor of water transparency in the China Sea by using satellite remote sensing. Engineering Science (in Chinese), 6(9): 33–37

Healey F P, Hendzel L L. 1980. Physiological indicators of nutrient deficiency in lake phytoplankton. Can J Fish Aquatic Sci, 37(3): 442–453

Hickox R, Belkin I, Cornillon P, et al. 2000. Climatology and seasonal variability of ocean fronts in the East China, Yellow and Bohai seas from satellite SST data. Geophysical Research Letters, 27(18): 2945–2948

Hu Dunxin. 1984. Upwelling and sedimentation dynamics: I. The role of upwelling in sedimentation in the Huanghai Sea and East China Sea—A description of general features. Chinese Journal of Oceanology and Limnology, 2(1): 12–19

Hu Minghui, Yang Yiping, Xu Chunling, et al. 1990. Phosphate limitation of phytoplankton growth in the Changjiang estuary. Acta Oceanol Sin, 9(3): 405–411

Huisman J, Thi N N P, Karl D M, et al. 2006. Reduced mixing generates oscillations and chaos in the oceanic deep chlorophyll maximum. Nature, 439(7074): 322–325

Joseph L, Villareal T A. 1998. Nitrate reductase activity as a measure of nitrogen incorporation in Rhizosolenia Formosa (H. Peragallo): internal nitrate and diel effects. J Exper Mar Biol Ecol, 229(2): 159–176

Klausmeier C A, Litchman E. 2001. Algal games: the vertical distribution of phytoplankton in poorly mixed water columns. Limnology and Oceanography, 46(8): 1998–2007

Li Furong. 1995. On the relationship between the distribution of dissolved oxygen and water masses in the Yellow Sea and East China Sea late in spring. Journal of Ocean University of Qingdao (in Chinese), 25(2): 255–263

Liu K K, Atkinson L, Quiñones R, et al. 2010. Carbon and Nutrient Flux-

es in Continental Margins: A Global Synthesis. Berlin: Springer, 741

Liu K K, Peng T H, Shaw P T, et al. 2003. Circulation and biogeochemical processes in the East China Sea and the vicinity of Taiwan: an overview and a brief synthesis. Deep-Sea Research Part II: Topical Studies in Oceanography, 50(6–7): 1055–1064

Lu Saiying, Ge Renfeng, Liu Lihui. 1996. The seasonal changes and physical nutrition salt waters of the East China Sea shelf transport law. Acta Oceanologica Sinica (in Chinese), 18(5): 41–51

Luo Minbo, Lu Jianjian, Wang Yunlong, et al. 2007. Horizontal distribution and dominant species of phytoplankton in the East China Sea. Acta Ecologica Sinica (in Chinese), 27(12): 5076–5085

Qi Jianhua, Li fengqi, Su yusong. 1991. Fuzzy discrimination and analysis of the spring water masses in Yellow Sea and East China Sea. Journal of Ocean University of Qingdao (in Chinese), 21(2): 13–20

Qu Tangdong, Hu Dunxin. 1993. Upwelling and sedimentation dynamics: II. A simple model. Chinese Journal of Oceanology and Limnology, 11(4): 289–295

Quan Qi, Mao Xinyan, Yang Xiaodan, et al. 2013. Seasonal variations of several main water masses in the Southern Yellow Sea and East China Sea in 2011. Journal of Ocean University of China, 12(4): 524–536

Son S, Yoo S, Noh J H. 2006. Spring phytoplankton bloom in the fronts of the East China Sea. Ocean Science Journal, 41(3): 181–189

Tang Danling, Di Baoping, Wei Guifeng, et al. 2006. Spatial, seasonal and species variations of harmful algal blooms in the South Yellow Sea and East China Sea. Hydrobiologia, 568(1): 245–253

Tawara S, Yamagata T. 1991. Seasonal formation of bottom water in the Yellow Sea and its interannual variability. Umi to Sora, 66: 273–282

Wang Baodong. 2003. Nutrient distributions and their limitation on phytoplankton in the Yellow Sea and the East China Sea. The Journal of Applied Ecology, 14(7): 1122–1126

Yanagi T, Shimizu T, Matsuno T. 1996. Baroclinic eddies south of Cheju Island in the East China Sea. Journal of Oceanography, 52(6): 763–769

Yu Haicheng, Xian Weiwei. 2009. The environment effect on fish assemblage structure in waters adjacent to the Changjiang (Yangtze) River estuary (1998–2001). Chinese Journal of Oceanology and Limnology, 27(3): 443–456

Yu Fei, Zhang Zhixin, Diao Xinyuan, et al. 2006. Analysis of evolution of the Huanghai Sea Cold Water Mass and its relationship with adjacent water masses. Haiyang Xuebao (in Chinese), 28(5): 26–34

Zhou Peiqiang, Sun Yueyan, Zhao Jisheng. 1990. A preliminary analysis of temperature and salinity in the sea RPEA near the Yangtse River mouth and ChlJuDo. Journal of Ocean University of Qingdao (in Chinese), 20(3): 49–55